Separation Science and Technology
Publication details, including instructions for authors and subscription information:
http://www.informaworld.com/smpp/title~content=t713708471

Operating Characteristics of Acoustically Driven Filtration Processes for Particulate Suspensions

Daniel H. Hill[a]; Donald L. Feke[b]
[a] Procter & Gamble, Mason, OH, U.S.A. [b] DEPARTMENT OF CHEMICAL ENGINEERING, CASE WESTERN RESERVE UNIVERSITY, CLEVELAND, OHIO, USA

Online publication date: 13 June 2000

To cite this Article Hill, Daniel H. and Feke, Donald L.(2000) 'Operating Characteristics of Acoustically Driven Filtration Processes for Particulate Suspensions', Separation Science and Technology, 35: 9, 1363 — 1375
To link to this Article: DOI: 10.1081/SS-100100229
URL: http://dx.doi.org/10.1081/SS-100100229

SEPARATION SCIENCE AND TECHNOLOGY, **35**(9), pp. 1363–1375, 2000

Operating Characteristics of Acoustically Driven Filtration Processes for Particulate Suspensions

DANIEL H. HILL* and DONALD L. FEKE†
DEPARTMENT OF CHEMICAL ENGINEERING
CASE WESTERN RESERVE UNIVERSITY
CLEVELAND, OHIO 44106-7217, USA

ABSTRACT

Operating characteristics for an ultrasonically assisted filtration technique applicable to micron to millimeter-sized particles suspended in liquid have been studied. The technique uses a highly porous filtration medium having pores up to two orders of magnitude larger than the particles being collected. When a resonant ultrasonic standing wave field is applied to the medium, the particles become trapped on the elements comprising the porous medium or within its pores. The test suspension consisted of 325-mesh polystyrene particles in water. The porous medium was a polyester mesh containing 30 pores per inch (the nominal pore size is 847 μm). Filtration efficiencies ranging from 60 to 85% have been observed. The effect of flow configuration on filtration efficiency and two approaches for cleaning of the mesh have been examined.

Key Words. Acoustic; Ultrasonic; Separation; Filtration; Particle

INTRODUCTION

Many chemical processes involve multiphase systems consisting of a liquid phase in contact with fine particles. Examples of such uses are catalyzed reaction processes, food processing, and recycling operations. Sometimes the motivation for using fine particles is the large surface-area-to-volume ratio associated with the size of the solid phase. The lower limit on particle size is

* Present address: Procter & Gamble, Mason, OH, USA.
† To whom correspondence should be addressed.

reached when postprocess separation of fluid and solid becomes prohibitively difficult or expensive. Consequently, there is demand for efficient and inexpensive means to separate fine particles from liquids. Recovery of either the fluid or the solid product, or satisfying environmental regulations, can be an impetus for such an operation.

Conventional separation techniques for fluid-particle systems fall into two categories (1). Settlers and centrifuges are examples of processes that rely on a density difference between particle and fluid. Techniques such as filtering, screening, and sieving rely on a difference in size between particles and the molecules of the suspending medium. With decreasing particle size, however, density-based separation becomes slower and more difficult. Likewise, size-based separation methods are prone to clogging, caking, and high pressure drops with decreasing particle size.

In addition to size- and density-based separation techniques, methods relying on application of external magnetic and electrostatic fields are practiced. These methods require that the particles be susceptible to the external fields. A difference in interfacial chemistry plays an important role in the flotation separation method. All of these techniques, however, are narrow in their applicability, and cannot be used for many materials.

In the past few decades the ability of acoustic waves to affect the motion and position of small particles has been explored (2–13). Acoustic separation techniques possess none of the disadvantages of conventional separation techniques, and require relatively low power. In addition to separation of particle and fluid, the application of standing waves to fluid-filled chambers has led to applications such as size-based fractionation of particles (14–16), compressibility-based fractionation (17), and retention of biological cells (18–20). The ultrasonic approach to solid–liquid separation is attractive, due both to its applicability to a wide range of particle-fluid systems and its potential success and applicability to particles in the micron to millimeter-size range.

With most of the previously reported ultrasonic separation methods, scale-up to industrial capacity is difficult, if not impossible. These techniques can require very precise control of fluid flow over small dimensions (disallowing a large throughput) or pseudostanding waves (8) to transport the collected particles relative to its suspending fluid (which is difficult to achieve in large-scale equipment).

In previous work (21) a separation technique that utilizes ultrasonic standing waves in conjuction with a highly porous medium has been reported. The medium has pores up to two orders of magnitude larger than that of the particles to be collected. However, the application of the ultrasonic field to the porous medium enables it to entrap particles, allowing clarified fluid to exit the chamber. In this paper we report some additional studies that focus on scale-up, long-term operation, flow geometry, and medium regeneration methods.

In order to begin to evaluate the potential for process scale-up, for this work we designed an acoustic separation chamber that had a significantly higher internal volume (approximately 280 cm^3) than used in any previous work involving the application of acoustic fields to porous media known to us (35.4 cm^3) (21). Also, since long-term operation is a necessary attribute for commercial and/or large-scale usage, the ability of the acoustic filtration approach to yield consistent exit concentration was another characteristic explored in this work. At some point during processing the porous medium becomes saturated with solids and no further particle collection occurs. Therefore, for continuing usage, it would be necessary to regenerate the filtration medium before saturation occurs. The effectiveness of two regeneration approaches was studied.

BACKGROUND

The general approach in acoustic separation processes involves application of a low intensity, resonant acoustic field to chambers. The intensity of the sound field must be below the threshold for acoustic streaming and cavitation; otherwise acoustically driven fluid motions disrupt the separation effect. When a planar ultrasonic standing wave field is applied to a particle suspended in a liquid, the particle experiences a time-averaged force known as the primary acoustic force, F_{ac} (21). This force arises from density and compressibility differences between the particle and fluid. If the particle is modeled as a sphere, and its radius (R) is much smaller than the acoustic wavelength, the primary acoustic force in a one-dimensional resonant sound field is expressed as (8)

$$F_{ac} = 4\pi R^3 \kappa E_{ac} F \sin(2\kappa x) \tag{1}$$

Here, κ and E_{ac} are the wavenumber and energy density of the acoustic field, respectively, and x is the position in the fluid relative to an acoustic pressure antinode. Also, the acoustic contrast factor F is given by (17)

$$F = \frac{1}{3}\left[\frac{5\Lambda - 2}{1 + 2\Lambda} - \frac{1}{\sigma^2\Lambda}\right] \tag{2}$$

where Λ is the ratio of particle to fluid density and σ is the ratio of the longitudinal speed of sound in the particle relative to the speed of sound in the fluid. The effect of this force is that particles migrate to either the nodes or antinodes of the sound field. Suspensions with a positive value for F locate at the pressure nodes, while particles are collected at acoustic pressure antinodes for systems with a negative F.

Secondary acoustic forces (also known as Bjerknes forces) can also arise from the interaction of scattered sound fields. Secondary forces F_b, which can occur between particles, is given by (11)

$$F_b = [\kappa^2 E_{ac}/2\pi]\ [1 - \gamma_1/\gamma_f]\ [1 - \gamma_2/\gamma_f]\ [V_1 V_2/d^2] \tag{3}$$

Here, V_1 and V_2 are the volumes of the interacting particles, d is the separation distance between the centers of the particles, and γ_1, γ_2, and γ_f are the compressibilities of the particles and fluid, respectively. The secondary forces are usually much smaller than the primary force; however, the secondary forces can become significant with large particles and/or small values of d.

Secondary forces tend to agglomerate particles of similar materials. As described in subsequent sections, the current work incorporates a porous polyester mesh within the separation chamber. Secondary forces may also act between the suspended particles and elements of this mesh.

Primary and secondary acoustic forces individually or in combination result in collection of the small suspended particles within the polymer mesh. For example, suppose an element of the porous mesh is located at the node of the acoustic field, and positive acoustic contrast particles are present. If the primary acoustic force entrapping a particle within a nodal plane is greater than the hydrodynamic entraining force associated with the motion of the particle around this element of the mesh, then the flow field will be unable to dislodge the particle. Thus the mesh can act as a filter although it might have pore sizes much larger than the particle being retained. Additionally, secondary acoustic forces may result in the formation of chains and clusters of particles around and onto the elements of the porous mesh. Also, particle agglomerates larger than the necks between the pores may form within the mesh.

EXPERIMENTAL SETUP

Two rectangular lead zirconate titanate (PZT) transducers manufactured by American Piezo Ceramics, Inc. (APC 880 grade, fundamental frequency 320 kHz), measuring 10.60 × 5.48 × 0.69 cm, form two sides of a rectangular chamber. The internal dimensions of the chamber are 10.00 × 5.65 × 4.90 cm, giving an internal volume of approximately 277 cm^3. The two sides of the chamber housing the transducers are removable Plexiglas plates, held to the main body of the chamber by screws. Rubber overlays between the removable plates and the chamber ensure a sealed fit. The two long faces each possess two tubing ports, and one of the remaining faces has four (Fig. 1). The chamber is filled with consolidated polyester foam having 30 pores per inch (nominal pore size is 847 μm) and a porosity greater than 0.9. One transducer serves as an emitter, and the other acts as a reflector. The emitting transducer was powered at 1.246 MHz by a Krohn-Hite 2100A signal generator and an ENI Model 2100L RF power amplifier. A Clarke Hess Model 2330 sampling V-A-W meter measured the electrical power consumption.

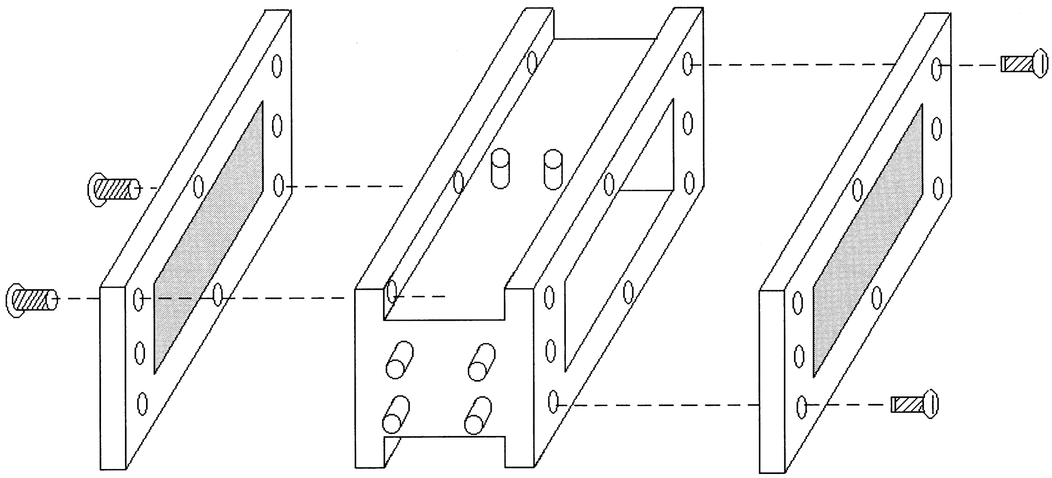

FIG. 1 Schematic of the acoustic chamber.

The material used for the test suspensions was 325-mesh polystyrene divinyl benzene particles dispersed in water using Triton X-100 surfactant to aid dispersion. This material had a broad size distribution (particle radius ranging from 10 to 40 μm) with a mean size of approximately 20 μm. This solid/liquid system has a positive acoustic contrast, resulting in particles collected in the acoustic nodes. The suspension was pumped through the chamber by a Masterflex 7520-00 peristaltic pump. Solids concentration was measured by converting light absorbance measurements from calibration charts made from suspensions of known concentration. The light absorbance was measured by a Milton Roy Spectronic 1001 Plus spectrophotometer in which the fluid travels through a Hellma Flow-Through cuvette. Absorbance measurements were written to a text file approximately every 4 seconds by means of a BASIC program run on a personal computer.

The acoustic forces acting on the particles depend on the particle size, the frequency of the signal, the acoustic contrast factor, and the acoustic energy density (15). An upper limit to the acoustic force exists. The wavelength of the signal must be much longer than the particle diameter for the particles to experience the primary acoustic force in the form described in the previous section; therefore, the frequency of the signal cannot violate this condition. In addition, at high acoustic energy levels, acoustic streaming occurs, disrupting the planar formation. For these reasons, optimal operating frequency and power levels were obtained experimentally. A frequency that resulted in strong, distinct planar formation (with no mesh installed within the chamber) was chosen. In addition, the power level was chosen so that it was high enough to maintain well-defined planes of particles, yet not high enough as to cause acoustic streaming.

EXPERIMENTS AND RESULTS

Visual Observations

In a fluid-filled chamber devoid of the porous medium, the planar formation was clearly visible. At a frequency of 1.246 MHz and with power input ranging from 7 to 12 W, the nodal planes of particles formed within 1 second of applying the acoustic field. Ideally, the planes would be perfectly vertical; however, some warping was observed near the top and bottom of the chamber. This effect was due to imperfections and edge effects of the ultrasonic standing wave field. At power levels above the normal operating range, acoustic streaming was observed. The acoustic streaming resembled a swirling flow.

Optical microscopy was used to observe the collection phenomena. In some cases the direct attachment of particles to the elements of the porous mesh could be observed. In other cases, aggregates of particles could be seen levitated within the pore space of the mesh.

The basic operating procedure for all the experiments was identical. The acoustic chamber, filled with the porous mesh, was initially filled with pure water. The transducer was then energized to the appropriate frequency and power input. Then the feed suspension was pumped through the chamber and the solids content of the exiting fluid was measured.

During all runs a thin layer of solids accumulated on the bottom of the chamber. This phenomenon was more prevalent when the ultrasonic standing wave was applied than when it was not. Close inspection revealed that most of the material within the medium was localized near the suspension entry port.

Proof of Principle and Long-Term Operation

Experiments were conducted in order to verify that the presence of an acoustic field did in fact increase the separation efficiency of the process. Each experiment was at least nine residence times (defined as the chamber volume divided by the suspension feed rate) in duration, with flow rates ranging from 35 to 55 cm^3/min. Figure 2 shows typical results.

For each experiment, data were plotted as dimensionless concentration (exit concentration C_e divided by feed concentration C_f) versus number of residence times. The collection efficiency η can be defined as

$$\eta = 1 - \frac{C_e}{C_f} \tag{4}$$

Thus, the smaller the value of C_e/C_f, the better the performance of the separation method. For each flow rate the application of acoustic waves to the chamber resulted in a substantial increase in collection efficiency compared to the performance with no acoustic field. Also note that more particles were re-

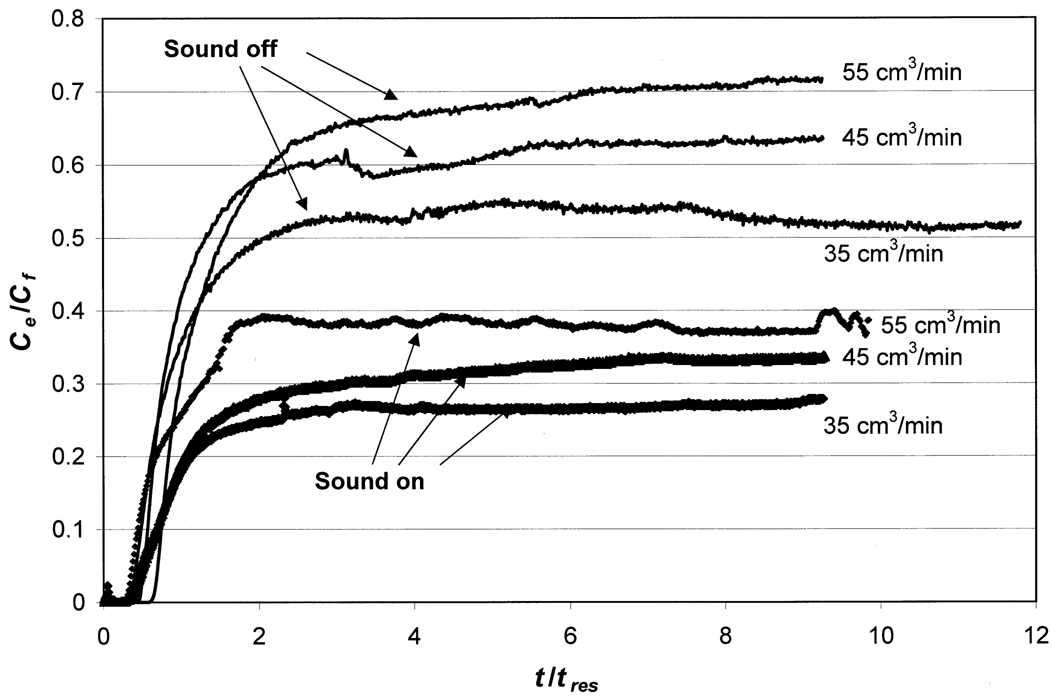

FIG. 2 Ratio of exit to feed concentration for 325-mesh polystyrene particles in water, 0.5 wt% at various suspension flow rates, through the acoustic chamber with no sound or a 1.246 MHz resonant sound field applied. Note that the application of the acoustic field results in significantly higher retention of solids by the mesh.

tained within the chamber at lower flow rates which can be attributed to the balance between acoustic forces acting to entrap the particles and the hydrodynamic forces trying to dislodge the particles from the porous mesh. In addition, the lower flow rates provide a longer interaction time between the particles and the acoustic field.

For a given set of operating conditions (frequency, power input, flow rate), the steady-state concentration was reproducible to within 5% of each other for five sets of data. Variations in feed concentration (0.3 to 0.6 wt%) had no effect on the dimensionless exit concentration.

In all of the experiments the exit concentration rose above zero before one residence time had elapsed even though the chamber was initially filled with only water. This indicates that the flow was not distributed uniformly throughout the acoustic chamber, and this is reasonable since only one feed port was used. The measurements of the effluent concentration as a function of time can also be affected by Taylor dispersion (22) that can occur in the tubing between the exit port of the acoustic chamber and the spectrophotometer. This was confirmed by control experiments in which suspension was pumped directly into the spectrophotometer.

In order to verify the reliability of these measurements, a material balance comparing the known amount of solute in the feed suspension to the sum of the solute exiting the chamber and the amount of solute retained within the chamber was performed. The error in the calculated particle mass and the actual particle mass was typically 5.5%, which illustrates that the measuring technique is valid.

Unlike the previous studies (21), no saturation phenomena were observed in these experimental trials even after operating the chamber continuously for a duration of over 40 residence times. There are several possible reasons why saturation was not observed during the current work. The combination of a much lower applied electric power (7–12 W) than was used in past work (Gupta used 20–50 W) and a larger acoustic chamber used in this work results in a lower acoustic energy density within the chamber. This makes the system less prone to acoustic streaming which can disrupt the collection phenomena.

Flow Geometry

It was expected that by adding complexity to the internal flow geometry of the chamber, thereby increasing the overall path length for flow, the operating efficiency of the acoustic separation would be enhanced. For this reason, three flow different configurations were explored (see Fig. 3). For flow geometries described as “vertical multipass,” a plastic divider is inserted at the bottom the chamber, parallel to the direction of flow. For systems referred to as “horizontal multipass,” the feed suspension enters at one end of the chamber and exist at the same end. In this case there is a horizontal plastic divider inserted within the chamber. The “single pass” geometry lacks any flow dividers; the feed enters the bottom of the chamber and exits the top.

With more intricate flow patterns the probability that a particle will encounter a fiber of the medium and become trapped increases; however, the higher linear velocity created by the smaller cross-sectional areas of the multipass geometries increases the hydrodynamic force working to overcome the acoustic forces. As expected, the efficiency of the operation increased with decreasing flow rate. The data for these experiments are presented as Figs. 4 and 5.

Both of the multipass geometries seem to outperform the single pass at similar flow speeds, with the horizontal configuration yielding the best results. This may be in part due to the horizontal multipass having the longest path length from entrance to exit. The coupling of long sideways flow and short elevation increase with the horizontal multipass results in more effective separation. Agglomerated particles may not be able to overcome the height requirement of the flow barrier. However, a layer of settled particles was visible on both flat surfaces of the horizontal multipass scheme, as well as flat surfaces for the other flow systems.

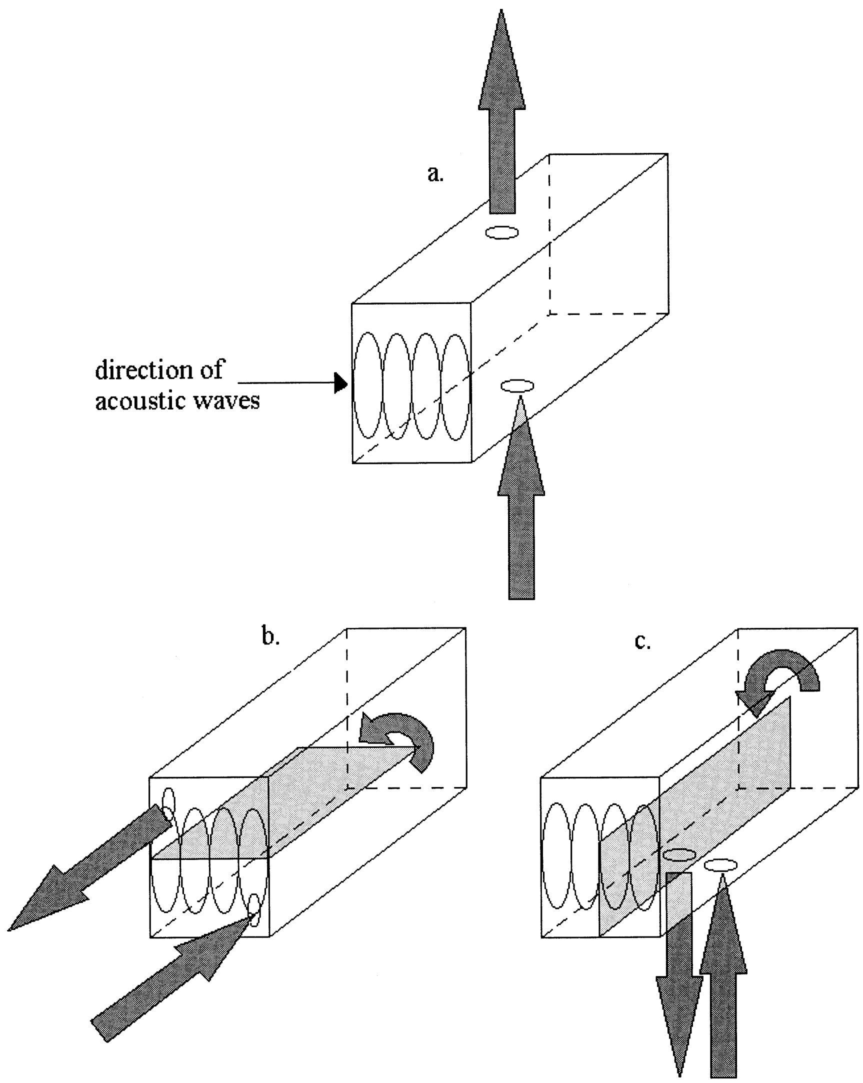

FIG. 3 Schematic of various flow geometries: (a) single pass; (b) horizontal multipass; (c) vertical multipass.

Another reason the horizontal fared better than the vertical flow configuration may lie in the orientation of the flow barriers. The barriers are made of plastic and are held in place and sealed with adhesive tape. The placement of the barrier for the vertical arrangement necessitates the sound waves traveling through the barrier, while in the horizontal geometry, little or no additional resistance to the propagation of the sound waves is caused by the barrier. The vertical barrier may be scattering or reflecting the sound waves, leaving no planar formation in half of the chamber. Although the precise mechanism for increased separation within more complex flow geometries is unclear, it is ev-

Marcel Dekker, Inc.
270 Madison Avenue, New York, New York 10016

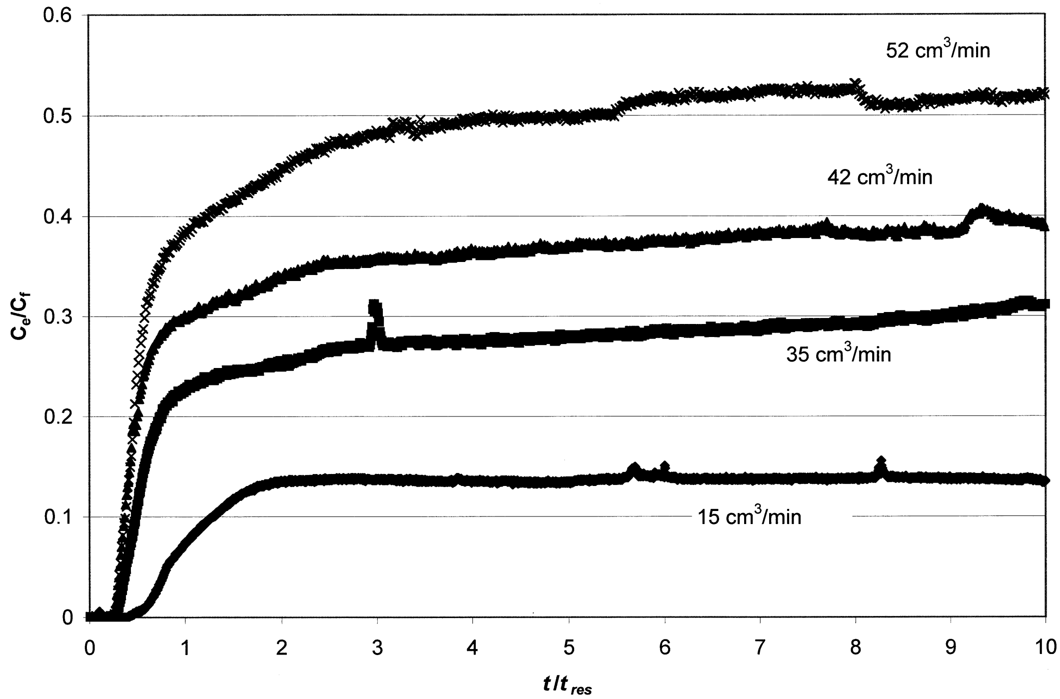

FIG. 4 Ratio of exit to feed concentration for 325-mesh polystyrene particles in water, 0.5 wt% at various suspension flow rates, through the acoustic chamber in a vertical multipass configuration with a 1.246 MHz resonant sound field applied.

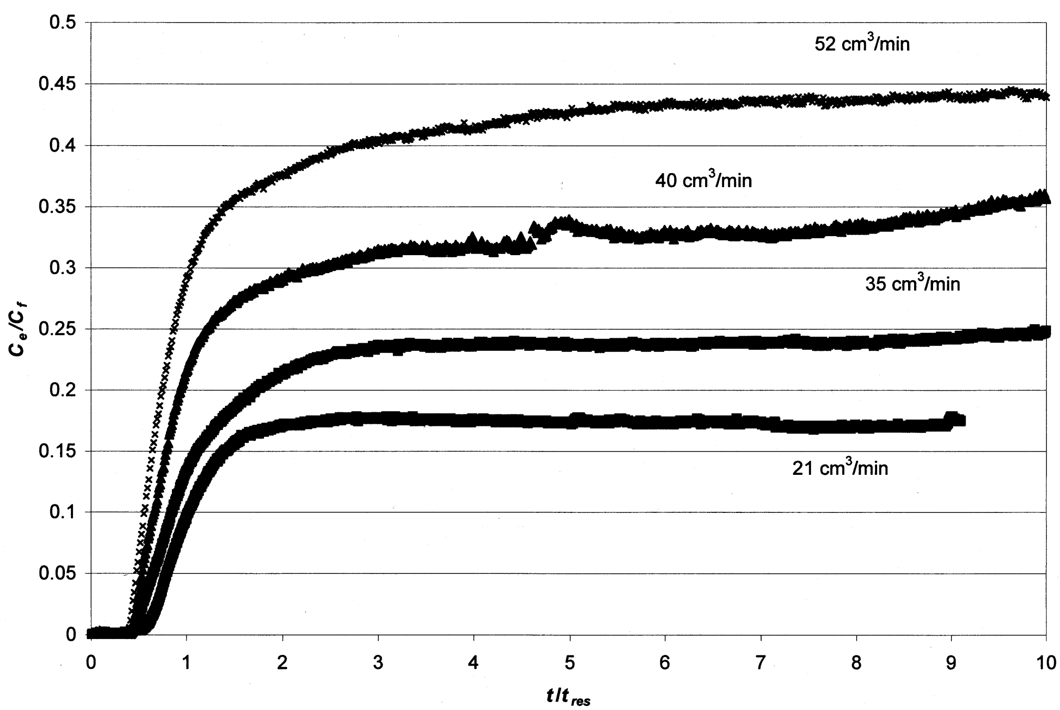

FIG. 5 Ratio of exit to feed concentration for 325-mesh polystyrene particles in water, 0.5 wt% at various suspension flow rates, through the acoustic chamber in a horizontal multipass configuration with a 1.246 MHz resonant sound field applied.

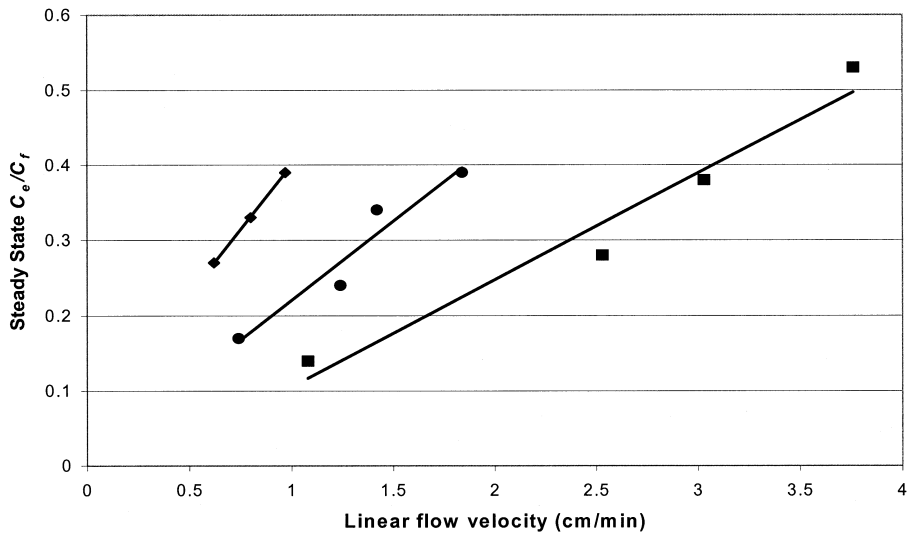

FIG. 6 Comparison of exit to feed concentration ratios for various flow velocities and geometries; feed concentration, 0.5 wt%; frequency, 1.246 MHz; single-pass (◆); horizontal multipass (■); vertical multipass (●).

ident that adding complexity to the flow field does result in a significant increase in separation efficiency.

In order to evaluate the effectiveness of the three geometric configurations, we compared the steady-state exit concentration as a function of the linear flow velocity through the mesh. Figure 6 displays these results, which shows that C_e/C_f is linear with respect to flow velocity for each of the configurations. This result is consistent with the notion that the hydrodynamic drag force is linear with flow speed and that the quality of the acoustic force is determined by the particular geometry used.

Medium Regeneration

Two methods for cleaning of the mesh (and recovery of the collected solids) were examined. One involved backflushing, which is performed by stopping the feed flow and pumping particle-free fluid at high flow rates through the mesh in the reverse direction. It is expected that the backflush fluid would carry with it a large portion of the trapped particles in a more concentrated form than the feed. The feed flow is then resumed, and this operation continues in a cyclic manner.

Experiments were performed using feed flow rates ranging from 30 to 50 cm^3/min in the single-pass chamber geometry. Each backflush period consisted of 1 minute. Because the backflush flow rate (130 cm^3/min) was very high compared to the feed flow rates, it was not necessary to terminate the sound field during the backflush operation. Typically, the concentration of particles in the backflush fluid ranged from approximately three times the feed concentration at the start of the backflush period to approximately half the feed concentration at the end of 1 minute of backflush. It was apparent that each backflush period emptied the chamber of nearly all the collected particles. Following the backflush period, the performance of the chamber resembled that observed using a clean mesh.

The second medium regeneration method studied involves alternating between operating the chamber with the sound on and with the sound off while the feed flow was maintained in the forward direction. For these experiments the acoustic source was turned off after five residence times had elapsed, at which time the exit flow was diverted and collected separately. The sound field was typically resumed after one residence time had lapsed. It was expected that the removal of the acoustic forces would allow the particles to escape the chamber, thus regenerating the separation potential of the porous medium. While the particle concentration in the exit stream did increase during the periods when the sound was terminated, the effect was not as effective as the backflushing technique. Additionally, the backflush method was found to empty the chamber of particles more quickly than the field termination approach.

CONCLUSIONS

Despite using a mesh having pores substantially larger than that of the suspended particles, the acoustic filtration technique was found to be effective. The exit concentration of the acoustic chamber remained fairly constant over extended periods of time, and separation efficiencies from 60 to 85% are reported. Despite operating for over 40 residence times, no saturation effect was ever observed. The horizontal multipass flow geometry outperformed the vertical multipass and single pass configurations. The efficiency of the acoustic separation is linear with respect to flow velocity for each flow-geometry studied. Backflushing the mesh proved to be a better method for regenerating the system mesh than did the approach of periodically terminating the acoustic field to release the particles.

Since the pore size of the medium is orders of magnitude larger than the particles, virtually no pressure drop is created by this filtration approach. This makes the acoustic separation process distinct from conventional filtration techniques. The acoustic process possesses a wide scope of applicability, relying only on compressibility and density differences between solid and liquid as a driving force. These factors, combined with the relatively low power requirement of this method, make acoustically enhanced solid/liquid separation an attractive option for separation applications.

ACKNOWLEDGMENT

The authors are grateful to Nestlé R & D for their support of this work through a Nestlé fellowship.

REFERENCES

1. A. Rushton, S. Ward, and R. Holdich, *Solid–Liquid Filtration and Separation Technology*, VCH Publishers, New York, NY, 1996.
2. S. Woodside, B. Bowen, and R. Piret, *AIChE J.*, *43*(7), 1727 (1997).
3. K. Yasuda, K. Takeda, and S. Umemura, *Jpn. J. Appl. Phys.*, *35*, 3295 (1996).
4. M. Bekker, J. Meyer, L. Pretorius, and D. Van Der Merwe, *Water Res.*, *31*(10), 2543 (1997).
5. G. Whitworth, M. Grundy, and W. Coakley, *Ultrasonics*, *29*, 439 (1991).
6. K. Higashitani, M. Fukushima, and Y. Matsuno, *Chem. Eng. Sci.*, *36*, 1877 (1981).
7. K. Yosioka and Y. Kawasima, *Acustica*, *5*, 167 (1955).
8. T. Tolt and D. Feke, *Chem. Eng. Sci.*, *48*(3), 527 (1993).
9. K. Yasuda, S. Umemura, and K. Takeda, *Jpn. J. Appl. Phys.*, *34*, 2715 (1995).
10. L. Gor'kov, *Sov. Phys. Dokl.*, *6*, 773 (1962).
11. R. Apfel, *Am. J. Phys.*, *56*, 726 (1988).
12. L. King, *Proc. R. Soc.*, *A147*, 212 (1934).
13. E. Benes, F. Hager, W. Bolek, and W. Groschl, *Proc. Ultrasonics. Int. Conf.*, p. 167 (1991).
14. Z. Mandralis and D. Feke, *Chem. Eng. Sci.*, *48*(23), 3897 (1993).
15. Z. Mandralis and D. Feke, *AIChE J.*, *39*(2), 197 (1993).
16. D. Johnson and D. Feke, *Sep. Technol.*, *5*, 251 (1995).
17. S. Gupta, D. Feke, and I. Manas-Zloczower, *Chem. Eng. Sci.*, *50*(20), 3275 (1995).
18. N. Baker, *Nature*, *239*, 398 (1972).
19. T. Gaida, O. Doblhoff-Dier, K. Strutzenberger, H. Katinger, W. Burger, M. Groschl, B. Handl, and E. Benes, *Biotechnol. Prog.*, *12*, 73 (1996).
20. R. Allman and T. Coakley, *Bioseparation*, *4*, 29 (1994).
21. S. Gupta and D. L. Feke, *AIChE J.*, *44*(5), 1005 (1998).
22. G. Taylor, *Proc. R. Soc.*, *A219*, 186 (1953).

Received by editor July 12, 1999
Revision received November 1999